21. Ribo M, Molina CA, Montaner J, *et al.* Acute hyperglycemia state is associated with lower tPA-induced recanalization rates in stroke patients. *Stroke* 2005; **36:** 1705–1709.
22. Kimura K, Iguchi Y, Shibazaki K, *et al.* Early recanalization rate of major occluded brain arteries after intravenous tissue plasminogen activator therapy using serial magnetic resonance angiography studies. *Eur Neurol* 2009; **62:** 287–292.
23. Bang OY, Saver JL, Buck BH, *et al.* Impact of collateral flow on tissue fate in acute ischaemic stroke. *J Neurol Neurosurg Psychiatry* 2008; **79:** 625–629.

Stroke Incidence and Usage Rate of Thrombolysis in A Japanese Urban City: The Kurashiki Stroke Registry

Yasuyuki Iguchi, MD,* Kazumi Kimura, MD,* Keiichi Sone, MD,† Hiroshi Miura, MD,‡ Hiroshi Endo, MD,§ Sen Yamagata, MD,|| Hisashi Koide, MD,¶ Kenji Suzuki, MD,# Tomoichiro Kimura, MD,** Masaru Sakurai, MD,†† Nobuya Mishima, MD,‡‡ Kenji Yoshii, MD,*** Hiroyuki Fujisawa, MD,††† and Sunao Ebisutani, MD,‡‡‡ for the Kurashiki Stroke Registry investigators

Background: To investigate stroke incidence and rate of thrombolytic therapy in an urban city of around 500,000 residents. *Methods:* Patients suffering acute stroke in Kurashiki City (population 474,415) between March 2009 and February 2010 (inclusive) and admitted to 1 of 10 hospitals throughout the city were prospectively enrolled. *Results:* We enrolled patients with first-ever stroke (n = 763; men 415; median age 72 years) and first-ever/recurrent stroke (n = 1009; men 552; median age 73 years). Among first-ever strokes, 68% were cerebral infarctions, 23% were intracerebral hemorrhages, and 8% were subarachnoid hemorrhages. Crude incidences for first-ever stroke per 100,000 residents were 159.8 (95% confidence interval [CI] 148.4-171.1) for all strokes, 108.8 (95% CI 99.4-118.1) for cerebral infarction, and 36.5 (95% CI 31.0-41.9) for intracerebral hemorrhage. After adjustment using the world population model, age-adjusted incidences were 60.7 (95% CI 45.4-75.9) for all strokes, 38.4 (95% CI 26.3-50.5) for cerebral infarction, and 16.1 (95% CI 8.3-24.0) for intracerebral hemorrhage. Among 698 cases with first-ever and recurrent cerebral infarction, thrombolysis was administered for 31 (5%). Of 197 cerebral infarction patients admitted within 3 hours of onset, the thrombolysis rate was 16%. *Conclusion:* In this urban Japanese city, the age-adjusted incidence of first-ever stroke between March 2009 and February 2010 was 60.7 per 100,000 residents, which was relatively low compared with findings for other countries. Thrombolysis was given to approximately 5% of patients with acute ischemic stroke. **Key Words:** Cerebral hemorrhage—cerebral infarct—epidemiology—stroke incidence—thrombolysis.

The socioeconomic burden caused by stroke in both Japan and high-income Western countries is likely to grow as the populations age.[1] With regard to stroke incidence in Japan, we have been able to refer to a couple of ideal studies,[2-4] with the most recent revealing a stroke incidence of approximately 120 per 100,000 adjusted by

From the *Department of Stroke Medicine, Kawasaki Medical School; †Kurashiki City Public Health Center; ‡Kurashiki City Medical Society; §Department of Internal Medicine, Kurashiki Rehabilitation Hospital; ||Department of Neurosurgery, Kurashiki Central Hospital; ¶Department of Internal Medicine, Kurashiki Kinen Hospital; #Departments of Neurosurgery at Kurashiki Heisei Hospital; **Kojima Central Hospital; ††Tamashima Central Hospital; ‡‡Mizushima Central Hospital; ***Mizushima Kyodo Hospital; †††Fujisawa Neurosurgical Hospital; and ‡‡‡Ohji Neurosurgical Clinic, Kurashiki, Japan.

Received August 9, 2011; revision received September 14, 2011; accepted September 19, 2011.

Supported by Science Research Grants (2009) from the Kurashiki City Public Health Center, Japan.

Address correspondence to Yasuyuki Iguchi, MD, Department of Stroke Medicine, Kawasaki Medical School, 577 Matsushima, Kurashiki City, Okayama, 701-0192, Japan. E-mail: yigu@med.kawasaki-m.ac.jp.

1052-3057/$ - see front matter

doi:10.1016/j.jstrokecerebrovasdis.2011.09.015

the Japanese standard population model.[4] However, we are uncertain of equivalent data for stroke incidence adjusted by the world standard population model in comparison with findings for other districts. In addition, previous investigations have been conducted in rural districts with small populations (<100,000), and most patients had been diagnosed with stroke based on computed tomography (CT), not by magnetic resonance imaging (MRI).

Since the approval of intravenous (IV) recombinant tissue plasminogen activator (rt-PA) by the Japanese government in 2005, safety and efficacy of IV rt-PA from retrospective and observational surveillance in Japan have appeared similar to those reported by the National Institute of Neurological Disorders rt-PA Stroke Trial,[5,6] but no epidemiologic inspections of IV rt-PA use have been described, such as the usage rate of IV rt-PA per stroke patient in a Japanese urban city of 474,415 residents. In order to plan adequate health care for individuals suffering acute stroke in Japan, we established a prospective stroke register to determine approximate stroke incidence based on MRI and usage rate of IV rt-PA in Kurashiki City, a city in midwestern Japan able to provide a high level of specialized stroke care.

Methods

Kurashiki City, adjacent to Okayama City, is the second largest community (covering 354.7 km^2) in Okayama Prefecture in midwestern Japan. The population of the city has been stable for several years (2009 population 474,415; men 232,244) and has been shown to be representative of a medium-sized Japanese city.[7]

Study Protocol and Stroke Ascertainment

We used Kurashiki Stroke Registry investigators from the Kurashiki City Public Health Center, Kurashiki City Medical Society, 2 comprehensive stroke centers, and 8 primary stroke centers to collect the data. Acute stroke patients who were treated within 7 days of onset at one of these 10 stroke centers were prospectively registered between March 2009 and February 2010. Paramedics in the Kurashiki City emergency medical service transferred possible acute stroke patients to these 10 stroke centers. We had already established an excellent consultation system between stroke centers and outpatient clinics, and consequently acute stroke patients who went to an outpatient clinic, with or without a stroke specialist, were referred to one of these 10 stroke centers.

All data were recorded, including clinical background (gender, age, and cohabitation status), vascular risk factors (history of hypertension, diabetes mellitus, dyslipidemia, and smoking), alcohol consumption, atrial fibrillation, past history of illness (stroke and ischemic heart disease), interval from onset to stroke center, method of admittance (ambulance transference), diagnosis of cerebrovascular disease (cerebral infarction, intracerebral hemorrhage, and subarachnoid hemorrhage), use of IV rt-PA based on previously published criteria,[8] and in-hospital death. The diagnosis of stroke within 7 days of onset was determined on the basis of the neurologic examination. In principle, stroke was defined as a focal neurologic deficit persisting for >24 hours, classified into categories of cerebral infarction, intracerebral hemorrhage, subarachnoid hemorrhage, or other/unknown. Neuroimaging including MRI was performed for all stroke patients. If contraindicated, CT was used. Subjects who died within 24 hours of symptom onset and had evidence of stroke on neuroimaging were also included as stroke cases. After investigators recorded the data on check sheets, these sheets were sent to the central office of the Kurashiki Stroke Registry at the Kurashiki City Public Health Center. The protocol for this investigation was approved by the ethics committee of Kawasaki Medical School.

Statistical Analysis

We calculated the gender- and age-specific rates of first-ever stroke (all subtypes of stroke, cerebral infarction, and intracerebral hemorrhage) per 100,000 residents of Kurashiki City after categorizing all cases into 17 age groups; <10, 10-14, 15-19, 20-24, 25-29, 30-34, 35-39, 40-44, 45-49, 50-54, 55-59, 60-64, 65-69, 70-74, 75-79, 80-84, and ≥85 years. We also analyzed the first-ever stroke incidence using the age distribution of the Japanese population from the 2005 census (Japanese model population 127,767,000),[9] the European standard population model, and the Segi standard population model (Segi model) using the direct method.[10] Direct method is the adjustment of crude rate to eliminate the effect of differences in population age structures when comparing crude rates for different periods of time, different geographic areas, and/or different population subgroups, as follows:

$$SR = (SUM(ri * Pi))/SUM\ Pi$$

where SR is the age-adjusted rate for the population being studied, ri is the age group–specific rate for age group i in the population being studied, and Pi is the population of age group i in the standard population.

The standard population used for purposes of international comparisons is generally the Segi model. Five-year age groups should normally be used (eg, <10, 10-14, 15-19...80-84, and 85). Because the age distribution was quite different between the Japanese population and the Segi standard model (eg, 15% of >70 years old in Japanese population *v* 4% in the Segi model), age-adjusted incidence by Segi model is extremely lower than crude incidence, especially in a disease occurring in elder residents. The 95% confidence interval (CI) was calculated for all incidence rates.

We compared age-adjusted incidences of all strokes,[1,4,11-24] cerebral infarctions,[1,4,16,24] and intracerebral

hemorrhages[1,4,16,24] between the present and previous reports. We referred to the age-adjusted incidence based on the Segi model and the average incidence according to the incomes of different countries as described in a 2009 systematic review.[1] We also calculated the usage rate of IV rt-PA per all cerebral infarctions and hyperacute cerebral infarction within 3 hours of onset.

Significant trends were examined using the Chi-square and the Mann–Whitney *U* tests. Statistical analyses were performed using PASW statistics software (version 18.0; SPSS, Inc, Chicago, IL). $P < .05$ was considered statistically significant.

Results

Between March 2009 and February 2010, the number of stroke patients hospitalized in the 10 facilities was 1009, including first-ever and recurrent stroke patients (men 552; median age 73 years; 25th-75th percentile; 64-80 years) among 474,415 residents. Of these 1009, there were 763 cases of first-ever stroke (men 415; median age 72 years; 25th-75th percentile; 62-80 years; Table 1). Male patients were significantly younger than female patients (first-ever and recurrent stroke 70 years for men *v* 76 years for women [$P < .001$]; first-ever stroke 69 years for men *v* 75 years for women [$P < .001$]). Diabetes, smoking, and alcohol consumption were more frequently seen in men than women. The 763 cases of first-ever stroke included 516 (68%) cerebral infarctions (287 men) and 173 (23%) intracerebral hemorrhages (103 men). Thrombolysis was performed for 31 (5%) of the 698 first-ever/recurrent cerebral infarction cases, and these 31 comprised 16% of the 197 cases admitted within 3 hours of stroke onset. Among patients with first-ever stroke, 27 patients received thrombolysis (6% of first-ever cerebral infarctions and 19% of cerebral infarctions admitted within 3 hours of onset). The in-hospital case fatality rate was 6%. Admission was by ambulance for 85% of patients with subarachnoid hemorrhage and 72% of those with intracerebral hemorrhage. However, only 41% of cerebral infarction patients used emergency medical transfer by ambulance (Fig 1). Aerial transportation was used in 7 cases (5 cases of intracerebral hemorrhage and 2 cases of cerebral infarction).

Age- and gender-specific rates of first-ever stroke per 100,000 residents, particularly for cerebral infarction, gradually increased with advancing age (Fig 2). In all age groups, the rate of cerebral infarction was higher in men than women. The rate of intracerebral hemorrhage was slightly higher than that of cerebral infarction in residents <50 years old. However, among residents ≥50 years old, the rate of cerebral infarction rapidly increased with age in comparison with intracerebral hemorrhage.

Table 2 shows first-ever stroke incidence (all strokes, cerebral infarctions, and intracerebral hemorrhages per 100,000 residents) according to crude and age-adjusted models. The incidence of all strokes per 100,000 residents was 159.8 (95% CI 148.4-171.2) in the crude model, 151.4 (95% CI 127.3-175.5) in the Japanese model, and 60.7 (95% CI 45.4-75.9) in the Segi model. The incidences of cerebral infarction per 100,000 residents were 108.8 (95% CI 99.4-118.1), 103.3 (95% CI, 83.4-123.2), and 38.4 (95% CI 26.3-50.5), respectively, while those of intracerebral hemorrhage were 36.5 (95% CI 31.0-41.9), 34.5 (95% CI 23.0-46.0), and 16.1 (95% CI 8.3-24.0), respectively. Age-adjusted stroke incidences calculated using the Segi model were markedly lower than crude incidences in our series.

Compared with studies from the last decade, incidence of all stroke adjusted using the Segi model was lower in the present study than in previous studies, apart from the Takashima[4] (rural Japan; Fig 3) and Dijon[11] (France) studies. While incidences of cerebral infarction in Japan (Kurashiki City and Takashima) were lower than in all other regions worldwide, the incidence of intracerebral hemorrhage in Japan took a middle position between high- and low-income countries.

Discussion

Age-adjusted incidence of first-ever stroke in our cohort was 151.4 per 100,000 by the Japanese model and 60.7 per 100,000 by the Segi model. While these data resemble those from Takashima, Japan,[4] our result was relatively lower than findings from previous studies conducted over the last decade.[1,11-24] Two possible explanations may account for this difference. First, because stroke incidence tends to be associated with socioeconomic status or national income,[1] high-income countries may be more likely to implement adequate stroke prevention policies. Indeed, the incidence and mortality rates of cerebral infarction dramatically decreased in Japan for several decades in accordance with proper control of hypertension after World War II.[3,4,25-27] Second, we observed wide disparities in population numbers in each age group between the Japanese model and the Segi model. For instance, patients <40 years old comprised 46% of the population in the Japanese census and 68% in the Segi model,[9,10] and while the Japanese population model listed 15% as >70 years old, the Segi model listed only 4%.[9,10] Stroke incidence in Kurashiki City declined from 151.4 per 100,000 in the Japanese model to 60.7 per 100,000 in the Segi model, a similar tendency to that seen in the register of southern Italy.[14] Finally, more than 95% of stoke patients admitted to general outpatient clinics were constantly referred to 1 of 10 stroke centers in Kurashiki City. Nevertheless, some stroke cases with mild deficit might be excluded from our registration.

Compared with the age-adjusted incidence of cerebral infarction in Figure 3, incidences of intracerebral hemorrhage in both Kurashiki City and Takashima were relatively higher than those in other high-income

Table 1. *Clinical backgrounds of the 1009 stroke patients*

Variables	First-ever and recurrent stroke				First-ever stroke			
	All cases (n = 1009*)	Men (n = 552)	Women (n = 450)	*P* value	All cases (n = 763‡)	Men (n = 415)	Women (n = 341)	*P* value
Age (y), median (IQR)	73 (64-80)	70 (62-77)	76 (67-84)	<.001	72 (62-80)	69 (61-77)	75 (66-84)	<.001
Risk factors (%)								
Hypertension	74	72	76	.088	70	68	73	.121
Diabetes mellitus	27	32	21	<.001	23	28	17	.001
Dyslipidemia	28	26	30	.450	27	25	29	.505
Smoking	26	40	8	<.001	26	42	7	<.001
Alcohol consumption	41	61	15	<.001	42	64	15	<.001
Atrial fibrillation (%)	14	13	15	.545	13	12	14	.595
History (%)								
Ischemic heart disease	12	13	10	.251	11	12	9	.240
Living alone (%)	15	13	18	.053	16	15	19	.223
Onset to door within 3 hours (%)	39	39	39	.905	40	41	38	.740
Transferring by ambulance (%)	52	52	51	.817	54	55	53	.723
Diagnosis (n)								
All strokes, total	1003†	552	449		758§	415	341	
By age group (y)								
<15	1	0	1		1	0	1	
15-19	0	0	0		0	0	0	
20-24	0	0	0		0	0	0	
25-29	3	0	3		2	0	2	
30-34	4	3	1		4	3	1	
35-39	12	7	5		12	7	5	
40-44	9	8	1		8	7	1	
45-49	24	19	5		19	15	4	
50-54	33	21	12		28	17	11	
55-59	70	42	28		57	36	21	
60-64	110	70	40		88	60	28	
65-69	142	100	42		113	80	33	
70-74	150	83	66		103	48	54	
75-79	166	91	75		117	63	54	
80-84	130	67	63		92	47	45	
≥85	149	41	107		114	32	81	
Cerebral infarction (total)	698	395	301		516	287	227	
By age group (y)								
<25	0	0	0		0	0	0	
25-29	3	0	3		2	0	2	
30-34	3	2	1		3	2	1	
35-39	3	3	0		3	3	0	
40-44	1	1	0		1	1	0	
45-49	9	7	2		7	5	2	
50-54	20	13	7		16	10	6	
55-59	41	23	18		31	17	14	
60-64	64	46	18		51	38	13	
65-69	101	73	28		80	59	21	
70-74	118	70	47		77	39	37	
75-79	122	73	49		83	50	33	
80-84	95	54	41		70	39	31	
≥85	118	30	87		92	24	67	
Intracerebral hemorrhage, total	232	131	101		173	103	70	
By age group (y)								
<15	1	0	1		1	0	1	
15-19	0	0	0		0	0	0	
20-24	0	0	0		0	0	0	

(*Continued*)

Table 1. *(Continued)*

Variables	First-ever and recurrent stroke				First-ever stroke			
	All cases (n = 1009*)	Men (n = 552)	Women (n = 450)	*P* value	All cases (n = 763‡)	Men (n = 415)	Women (n = 341)	*P* value
25-29	0	0	0		0	0	0	
30-34	1	1	0		1	1	0	
35-39	4	3	1		4	3	1	
40-44	6	5	1		5	4	1	
45-49	14	11	3		11	9	2	
50-54	7	5	2		6	4	2	
55-59	20	14	6		17	14	3	
60-64	38	21	17		30	19	11	
65-69	31	22	9		24	17	7	
70-74	22	12	10		17	8	9	
75-79	34	16	18		25	11	14	
80-84	29	11	18		16	6	10	
≥85	25	10	15		16	7	9	
Subarachnoid hemorrhage, total	67	21	46		63	20	43	
Other or undetermined categories	6	5	1		6	5	1	
Thrombolysis (n, %)								
Ischemic stroke	31/698 (5)	18/395 (5)	13/301 (5)	.434	27/516 (6)	15/287 (6)	12/227 (6)	.877
Within 3 hours of onset	31/197 (16)	18/112 (17)	13/85 (16)	.552	27/144 (19)	15/80 (19)	12/64 (19)	1.000
Within 2 hours of onset	23/122 (19)	13/67 (20)	10/55 (19)	1.000	19/93 (21)	10/50 (20)	9/43 (21)	1.000
Within 1 hour of onset	5/46 (11)	2/23 (9)	3/23 (13)	1.000	5/39 (13)	2/19 (11)	3/20 (15)	1.000
In-hospital case fatality rate (%)	6	5	9	.031	6	5	9	.072

Abbreviation: IQR, interquartile range.
*In 1009 cases with first-ever and recurrent stroke, 7 cases were of unknown gender.
†Among 1009 cases, 1003 cases had age information. Two cases with cerebral infarction did not have gender information.
‡In 763 cases with first-ever stroke, 7 cases were of unknown gender.
§Among 763 cases, 758 cases had age information. Two cases with cerebral infarction did not have gender information.

countries.[1,4] This finding may be mainly related to ethnic factors, particularly those associated with Asian cohorts.[28] In fact, the rate of intracerebral hemorrhage resembled that of cerebral infarction in Kurashiki City residents <50 years old. We believe that maintaining normal blood pressure in younger residents may be important in preventing intracerebral hemorrhage.

To the best of our knowledge, this is the first Japanese investigation of the IV rt-PA usage rate in a midsize city. The frequency of thrombolytic therapy was 5% for cerebral infarction and 16% for cerebral infarction patients admitted within 3 hours of onset. Compared with previous studies conducted during the last decade,[29-34] our results revealed a higher usage rate of IV rt-PA, particularly for hyperacute stroke patients admitted within 3 hours of onset. The reason may be that Kurashiki City has a well-established medical system for acute stroke care. Regarding stroke advertisements, Japan Stroke

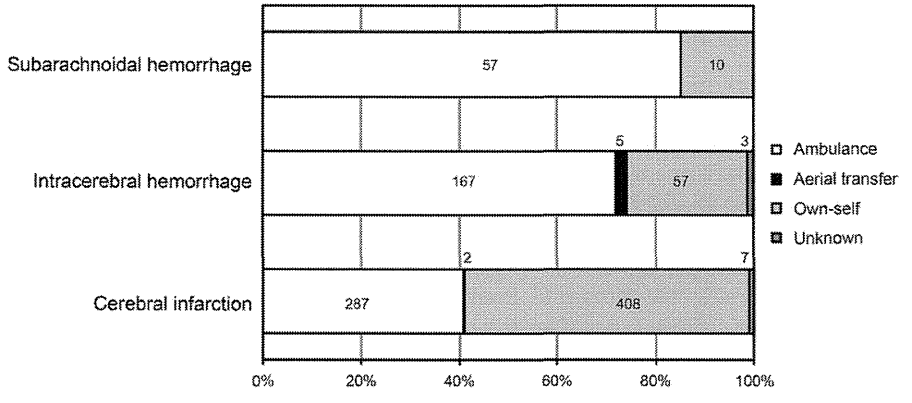

Figure 1. *Proportional frequency of transfer from site of onset to our facilities in terms of stroke subtypes.*

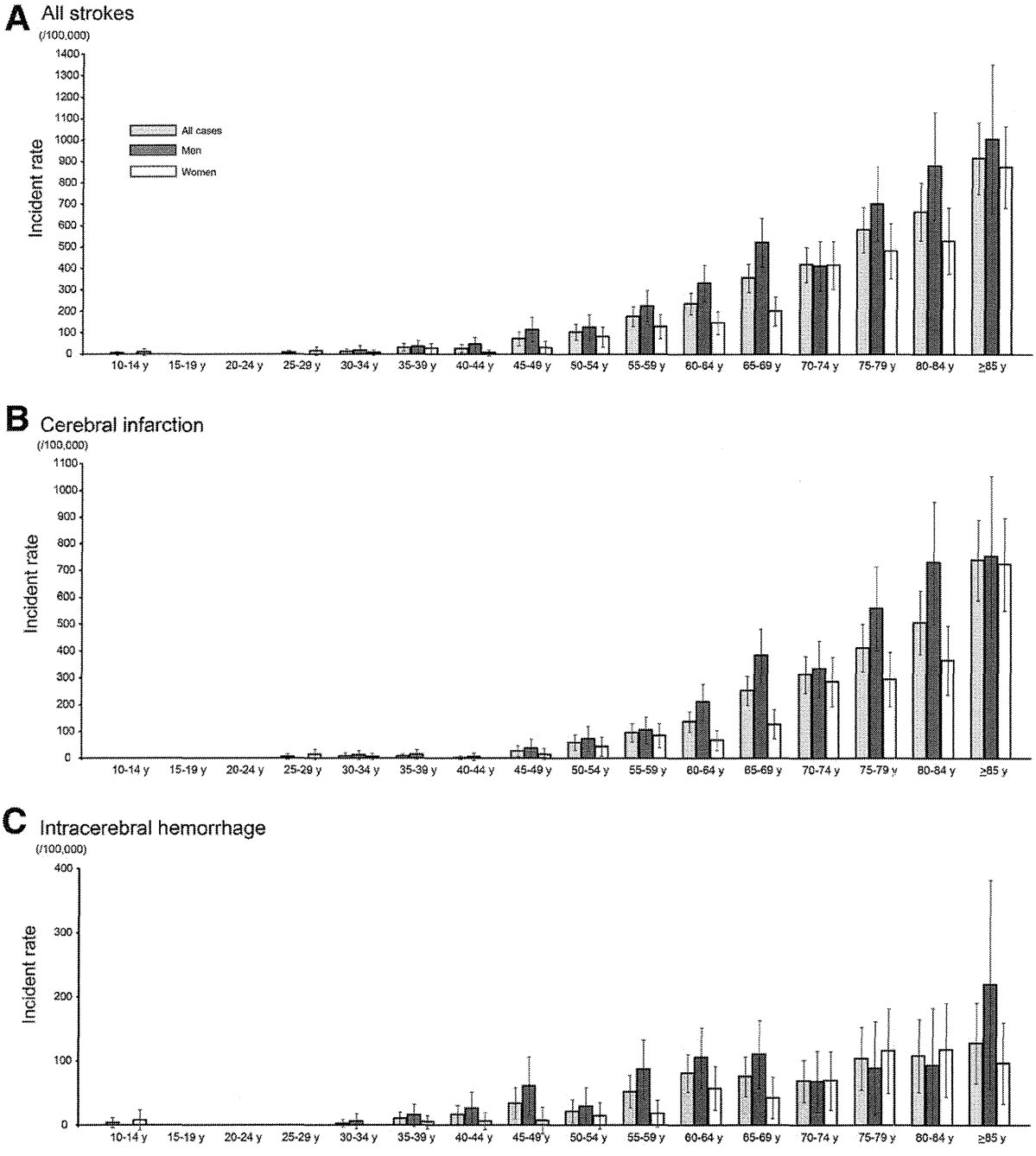

Figure 2. *Age- and sex-specific rates per 100,000 residents for first ever stroke* (A, *all strokes;* B, *cerebral infarction; and* C, *intracerebral hemorrhage).*

Association in Okayama Prefectural branch has undertaken an extensive education campaign on stroke knowledge for Kurashiki City residents using posters, television commercials, and special television programs presented by the public broadcasting station.[35] In the prehospital setting, paramedics always assess the patient with suspected stroke using the Kurashiki Prehospital Stroke Scale.[36] While transferring possible stroke patients, our community provides a direct communication system between paramedics and stroke specialists in 2 comprehensive stroke centers. Consequently, systematic prehospital stroke care seems likely to play an important role in achieving the high-usage rate of IV rt-PA.

The overall in-hospital case fatality rate was 6% for both all strokes and first-ever stroke. These results were not in line with previous reports describing a case fatality rate of 14% in the first 7 days[17] and from 10% to 38% at 28 days after onset.[11,37] Direct comparison of data between the present study and other investigations is not feasible, because the case-fatality rate depends on the

Table 2. *Incidence of first-ever stroke per 100,000 residents*

	All strokes (n = 758)	Cerebral infarction (n = 516)	ICH (n = 173)
Crude model (95% CI)	159.8 (148.4-171.1)	108.8 (99.4-118.1)	36.5 (31.0-41.9)
Japanese population model (95% CI)	151.4 (127.3-175.5)	103.3 (83.4-123.2)	34.5 (23.0-46.0)
Scandinavian population model (95% CI)	91.2 (72.5-109.9)	59.2 (44.2-74.3)	23.0 (13.6-32.4)
Segi population model (95% CI)	60.7 (45.4-75.9)	38.4 (26.3-50.5)	16.1 (8.3-24.0)

Abbreviations: CI, confidence interval; ICH, intracerebral hemorrhage.

initial stroke severity, age, and the observational interval from onset to outcome.[38] However, seen in the most favorable light, short-term mortality in present study seems lower than previously reported.[11,17,37]

Several limitations of the present study must be considered. First, the study only ran over a short period of time (1 year), with no data regarding any secular trends in stroke incidence. We were therefore unable to estimate stroke severity on admission using the National Institute of Health Stroke Scale and long-term outcomes at 3 months after onset. This may have affected our interpretation of the validity of acute stroke care in Kurashiki City. Second, we were unable to compare to our results to some ideal studies investigating Asian ethnic groups, because they restricted the generation of the study population to >40[39] or 25 to 74 years of age.[40]

In conclusion, age-adjusted incidence of first-ever stroke after government approval of thrombolysis was 60.7 per 100,000 residents in Kurashiki City, Japan. Thrombolysis was performed for 5% of cerebral infarction patients and 16% of cerebral infarction patients admitted within 3 hours of onset.

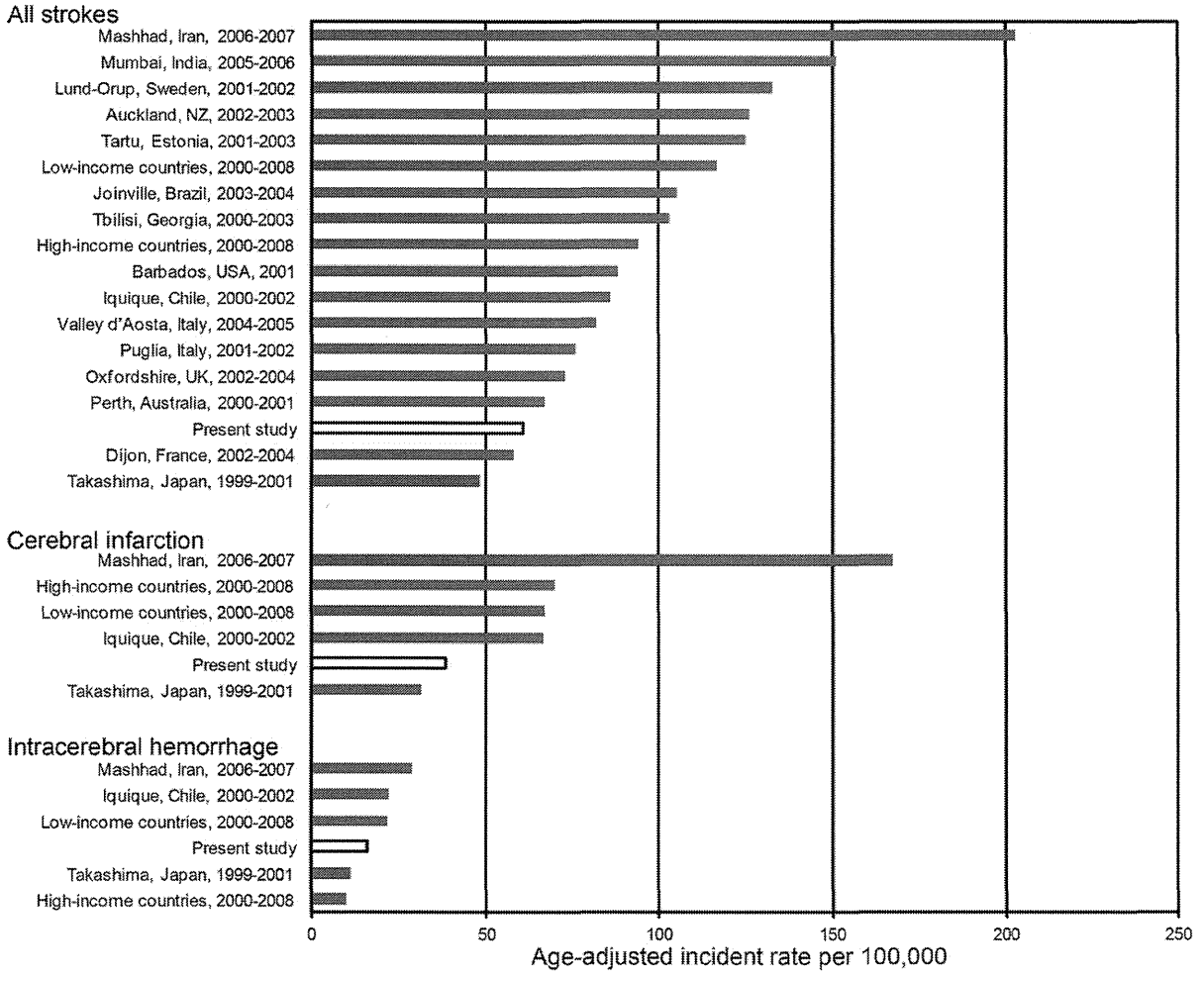

Figure 3. *Age-adjusted incidence of all strokes, cerebral infarction, and intracerebral hemorrhage as estimated by the present and previous studies from 2001 to 2010. All data were adjusted using the Segi standard population model.*

References

1. Feigin VL, Lawes CM, Bennett DA, et al. Worldwide stroke incidence and early case fatality reported in 56 population-based studies: A systematic review. Lancet Neurol 2009;8:355-369.
2. Tanaka H, Ueda Y, Date C, et al. Incidence of stroke in Shibata, Japan: 1976-1978. Stroke 1981;12:460-466.
3. Kubo M, Kiyohara Y, Kato I, et al. Trends in the incidence, mortality, and survival rate of cardiovascular disease in a Japanese community: The Hisayama study. Stroke 2003;34:2349-2354.
4. Kita Y, Turin TC, Ichikawa M, et al. Trend of stroke incidence in a Japanese population: Takashima Stroke Registry, 1990-2001. Int J Stroke 2009;4:241-249.
5. Toyoda K, Koga M, Naganuma M, et al. Routine use of intravenous low-dose recombinant tissue plasminogen activator in Japanese patients: General outcomes and prognostic factors from the SAMURAI register. Stroke 2009;40:3591-3595.
6. Tissue plasminogen activator for acute ischemic stroke. The National Institute of Neurological Disorders and Stroke rt-PA Stroke Study Group. N Engl J Med 1995;333:1581-1587.
7. Kurashiki city web site. Population, 2009. Available from http://www.city.kurashiki.okayama.jp/dd.aspx?itemid=32052#itemid32052. Accessed October 4, 2011.
8. Yamaguchi T, Mori E, Minematsu K, et al. Alteplase at 0.6 mg/kg for acute ischemic stroke within 3 hours of onset—Japan Alteplase Clinical Trial (J-ACT). Stroke 2006;37:1810-1815.
9. e-Stat web site. The population of Japan, Ministry of Internal Affairs and Communications. Available from http://www.e-stat.go.jp/SG1/estat/List.do?bid=000001008470&cycode=000001008470. Accessed October 4, 2011.
10. Ahmad O, Boschi-Pinto C, Lopez AD, et al. Age standardization of rates: A new WHO standard. Geneva: World Health Organization, 2001.
11. Benatru I, Rouaud O, Durier J, et al. Stable stroke incidence rates but improved case-fatality in Dijon, France, from 1985 to 2004. Stroke 2006;37:1674-1679.
12. Islam MS, Anderson CS, Hankey GJ, et al. Trends in incidence and outcome of stroke in Perth, Western Australia during 1989 to 2001: The Perth Community Stroke Study. Stroke 2008;39:776-782.
13. Rothwell PM, Coull AJ, Silver LE, et al. Population-based study of event-rate, incidence, case fatality, and mortality for all acute vascular events in all arterial territories (Oxford Vascular Study). Lancet 2005;366:1773-1783.
14. Manobianca G, Zoccolella S, Petruzzellis A, et al. Low incidence of stroke in southern Italy: A population-based study. Stroke 2008;39:2923-2928.
15. Corso G, Bottacchi E, Giardini G, et al. Community-based study of stroke incidence in the Valley of Aosta, Italy. CARe-cerebrovascular Aosta Registry: Years 2004-2005. Neuroepidemiology 2009;32:186-195.
16. Lavados PM, Sacks C, Prina L, et al. Incidence, 30-day case-fatality rate, and prognosis of stroke in Iquique, Chile: A 2-year community-based prospective study (PISCIS project). Lancet 2005;365:2206-2215.
17. Corbin DO, Poddar V, Hennis A, et al. Incidence and case fatality rates of first-ever stroke in a black Caribbean population: The Barbados Register of Strokes. Stroke 2004;35:1254-1258.
18. Tsiskaridze A, Djibuti M, van Melle G, et al. Stroke incidence and 30-day case-fatality in a suburb of Tbilisi: Results of the first prospective population-based study in Georgia. Stroke 2004;35:2523-2528.
19. Cabral NL, Goncalves AR, Longo AL, et al. Incidence of stroke subtypes, prognosis and prevalence of risk factors in Joinville, Brazil: A 2-year community based study. J Neurol Neurosurg Psychiatry 2009;80:755-761.
20. Vibo R, Korv J, Roose M. The Third Stroke Registry in Tartu, Estonia, from 2001 to 2003. Acta Neurol Scand 2007;116:31-36.
21. Anderson CS, Carter KN, Hackett ML, et al. Trends in stroke incidence in Auckland, New Zealand, during 1981 to 2003. Stroke 2005;36:2087-2093.
22. Hallstrom B, Jonsson AC, Nerbrand C, et al. Lund Stroke Register: Hospitalization pattern and yield of different screening methods for first-ever stroke. Acta Neurol Scand 2007;115:49-54.
23. Dalal PM, Malik S, Bhattacharjee M, et al. Population-based stroke survey in Mumbai, India: Incidence and 28-day case fatality. Neuroepidemiology 2008;31:254-261.
24. Azarpazhooh MR, Etemadi MM, Donnan GA, et al. Excessive incidence of stroke in Iran: Evidence from the Mashhad Stroke Incidence Study (MSIS), a population-based study of stroke in the Middle East. Stroke 2010;41:e3-e10.
25. Ueshima H. Trends in Asia. In: Marmot MG, Elliott P, eds. Coronary heart disease epidemiology: From aetiology to public health. 2nd ed. New York: Oxford University Press, 2005:102-112.
26. Ueshima H, Tatara K, Asakura S, et al. Declining trends in blood pressure level and the prevalence of hypertension, and changes in related factors in Japan, 1956-1980. J Chronic Dis 1987;40:137-147.
27. Ueshima H. Changes in dietary habits, cardiovascular risk factors and mortality in Japan. Acta Cardiol 1990;45:311-327.
28. van Asch CJ, Luitse MJ, Rinkel GJ, et al. Incidence, case fatality, and functional outcome of intracerebral haemorrhage over time, according to age, sex, and ethnic origin: A systematic review and meta-analysis. Lancet Neurol 2010;9:167-176.
29. Bateman BT, Schumacher HC, Boden-Albala B, et al. Factors associated with in-hospital mortality after administration of thrombolysis in acute ischemic stroke patients: An analysis of the nationwide inpatient sample 1999 to 2002. Stroke 2006;37:440-446.
30. Edwards LL. Using tPA for acute stroke in a rural setting. Neurology 2007;68:292-294.
31. Eriksson M, Jonsson F, Appelros P, et al. Dissemination of thrombolysis for acute ischemic stroke across a nation: Experiences from the Swedish stroke register, 2003 to 2008. Stroke 2010;41:1115-1122.
32. Heuschmann PU, Berger K, Misselwitz B, et al. Frequency of thrombolytic therapy in patients with acute ischemic stroke and the risk of in-hospital mortality: The German Stroke Registers Study Group. Stroke 2003;34:1106-1113.
33. Lindsberg PJ, Soinne L, Roine RO, et al. Community-based thrombolytic therapy of acute ischemic stroke in Helsinki. Stroke 2003;34:1443-1449.
34. Schumacher HC, Bateman BT, Boden-Albala B, et al. Use of thrombolysis in acute ischemic stroke: Analysis of the nationwide inpatient sample 1999 to 2004. Ann Emerg Med 2007;50:99-107.
35. Nakayama H. Brain attack project. Available from http://www.jsa-web.org/bap/bap.html. Accessed October 4, 2011.
36. Kimura K, Inoue T, Iguchi Y, et al. Kurashiki prehospital stroke scale. Cerebrovasc Dis 2008;25:189-191.
37. Sridharan SE, Unnikrishnan JP, Sukumaran S, et al. Incidence, types, risk factors, and outcome of stroke in

a developing country: The Trivandrum Stroke Registry. Stroke 2009;40:1212-1218.
38. Kimura K, Minematsu K, Kazui S, et al. Mortality and cause of death after hospital discharge in 10,981 patients with ischemic stroke and transient ischemic attack. Cerebrovasc Dis 2005;19:171-178.
39. Zhao D, Liu J, Wang W, et al. Epidemiological transition of stroke in China: Twenty-one-year observational study from the Sino-MONICA-Beijing Project. Stroke 2008;39:1668-1674.
40. Kubo M, Hata J, Doi Y, et al. Secular trends in the incidence of and risk factors for ischemic stroke and its subtypes in Japanese population. Circulation 2008;118:2672-2678.

ELSEVIER

Ultrasound in Med. & Biol., Vol. ■, No. ■, pp. 1–12, 2013

0301-5629/$ - see front matter

http://dx.doi.org/10.1016/j.ultrasmedbio.2012.11.011

● *Original Contribution*

COMPARATIVE STUDY OF STANDING WAVE REDUCTION METHODS USING RANDOM MODULATION FOR TRANSCRANIAL ULTRASONICATION

HIROSHI FURUHATA and OSAMU SAITO
Medical Engineering Laboratory, The Jikei University School of Medicine, Tokyo, Japan

(*Received* 14 *February* 2012; *revised* 9 *November* 2012; *in final form* 12 *November* 2012)

Abstract—Various transcranial sonotherapeutic technologies have risks related to standing waves in the skull. In this study, we present a comparative study on standing waves using four different activation methods: sinusoidal (SIN), frequency modulation by noise (FMN), periodic selection of random frequency (PSRF), and random switching of both inverse carriers (RSBIC). The standing wave was produced and monitored by the schlieren method using a flat plane and a human skull. The minimum ratio R_{SW}, which is defined by the ratio of the mean of the difference between local maximal value and local minimal value of amplitude to the average value of the amplitude, was 36% for SIN, 24% for FMN, 13% for PSRF, and 4% for RSBIC for the flat reflective plate, and it was 25% for SIN, 11% for FMN, 13% for PSRF, and 5% for RSBIC for the inner surface of the human skull. This study is expected to have a role in the development of safer therapeutic equipment. (E-mail: furuhata@jikei.ac.jp) © **2013 World Federation for Ultrasound in Medicine & Biology.**

Key Words: **Standing wave, Ultrasound, Skull, Random modulation, Sonotherapy.**

INTRODUCTION

Recent progress in transcranial ultrasonic therapeutic technologies has brought about a potential non-invasive treatment for brain tumors, blood-brain-barrier opening (Hynynen et al. 2006; Konofagou et al. 2012), and thrombolysis. Examples for the thrombolysis are high-intensity focused ultrasound (US) navigated by magnetic resonance imaging (MRI; Hynynen et al. 2001, 2006, 2007; Marsac et al. 2012), mild intensity focused ultrasound combined with a ultrasonic contrast agent, and sonothrombolysis with a defocused US beam (Daffertshofer et al. 2005). These new treatments have to overcome various adverse effects concerning US beam formation to realize widespread clinical application (Ammi et al. 2008; Azuma et al. 2004; Clement et al. 2005; Culp et al. 2005; Daffertshofer et al. 2002; Fry 1956; Fry and Fry 1960; Fry et al. 1981; Kawata et al. 2007; McDannold et al. 2010; Mikulik et al. 2006).

However, at present, biologic effects such as heating and cell damage by a standing wave (SW) on the human skull have not been completely solved from an acoustic point of view. Although the large-aperture transducer used in HIFU guided by MRI has been demonstrated not to induce a SW, the small-aperture transducers can produce a non-negligible SW (Song et al. 2012). The focused US treatment combined with a diagnostic ultrasonic transducer phased array has been reasonably solved. In particular, a single US sector scan probe, which was a laminated diagnostic phased array and mid-frequency therapeutic phased array, has exhibited the potential for use in target sonothrombolysis of the thrombus in the middle cerebral artery with the aid of the systemic rt-PA venous injection (Azuma et al. 2010). Nevertheless, a conventional transcranial sonothrombolysis approach with a defocused ultrasonic beam can induce SW adverse effects caused by the continuous wave as well as the burst wave (Baron et al. 2009; Daffertshofer et al. 2005; Pinton et al. 2012). Therefore, to solve the SW bio-effects from an acoustic point of view, we focused on the electric waveform driving the transducer and compared the spatial SW appearance, which does not depend on the 3-D formation of a phased array transducer.

Various methods of sending an electric signal to the ultrasonic transducer have been investigated for the purpose of SW reduction. Tang and Clement (2009, 2010) tried to reduce the SW and succeeded by using randomly modulated wave and random phase-shift keying (PSK), which introduces phase shifts into the driving signal for each time segment. (In the random PSK, the

Address correspondence to: Hiroshi Furuhata, The Jikei University School of Medicine, Medical Engineering Laboratory, 3-25-8 Nishi-shinbashi, Minato-ku, Tokyo 105-8461, Japan. E-mail: furuhata@jikei.ac.jp

phase shifts such as 0, $\frac{\pi}{2}$, π, and $\frac{3\pi}{2}$ are randomly ordered.). Based on the same concept (*i.e.*, that randomization is effective for the reduction of SWs), we investigate further and try to obtain more effective modulation methods—that is, a safer activation method for a transducer in transcranial US therapy. In this study, we present two new modulation methods and compare them with the frequency modulation by noise (FMN), which is used by Tang and Clement (2010). One of the new modulation methods involves the periodic selection of random frequency (PSRF), in which various random frequencies are chosen periodically. This is different from the frequency-shift keying used in digital communication in terms of the randomization of frequencies. The other method is random switching of both inverse carriers (RSBIC), in which the phase is reversed at a random time, which is different from binary PSK (the phase shifts for which are 0 or π) in terms of the random length of the segment.

The purpose of this article is to provide a comparative study of these three random modulation methods. Beginning by recalling the need to modulate the US beams and justifying the single reflection experiment, this article describes the experimental results obtained by comparing the three random modulation methods using the schlieren method. This result is significant regarding the application of these methods to safe transcranial ultrasonication for various noninvasive therapeutic methods without the appearance of SWs.

MATERIALS AND METHODS

Simplified SW estimation by 1-D multireflection

If a US wave is injected into the cranium, the wave will reflect from the inner wall of the cranium. The reflected waves can pass through the same region several times, and the acoustic intensity can be increased by phase matching in some regions and can be decreased in other regions. If the injected wave is sinusoidal, SWs are expected to arise for any size of skull and for any reflection time. As an example, we consider a 1-D propagation model in which plane waves propagate along the x-axis and two parallel reflective plates are placed at $x = 0$ and $x = L$. (The real skull bones are not parallel but have numerous small hills and valleys.) When a monochromatic wave having a wavelength of λ is injected at $x = 0$, the amplitude at position x ($0 < x < L$) is as follows:

$$A(x) = \sqrt{\frac{1+2R\cos\left(\frac{4\pi}{\lambda}(L-x)\right)+R^2}{1-2R^2\cos\left(\frac{4\pi L}{\lambda}\right)+R^4}} \qquad (1)$$

where R ($0 < R < 1$) is the reflective ratio. The amplitude depends on the position. In other words, there are hot and cold spots. Neither attenuation in the brain nor diffraction is taken into account in this model, although both attenuation in the brain and diffraction can occur in the real case.

We define the ratio R_{SW} as follows:

$$R_{SW} = \frac{A_{max} - A_{min}}{A_{mean}}, \qquad (2)$$

where A_{max}, A_{min} and A_{mean} are the maximum, minimum and mean of the amplitude, respectively.

Whereas the average amplitude A_{mean} characterizes the intensity of the waves, R_{SW} is related to the difference between hot and cold spots. In this model, the average amplitude and R_{SW} are given by:

$$A_{mean} = \frac{2}{\pi}\cdot\frac{1+R}{\sqrt{1-2R^2\cos\left(\frac{4\pi L}{\lambda}\right)+R^4}}\cdot E\left(\frac{2\sqrt{R}}{1+R}\right), \qquad (3)$$

$$R_{SW} = \pi\cdot\frac{R}{1+R}\cdot\frac{1}{E\left(\frac{2\sqrt{R}}{1+R}\right)}, \qquad (4)$$

where $E(\cdot)$ is the complete elliptic integral of the second kind. Whereas the average amplitude depends on L (in particular, the average amplitude is the largest if L is a multiple of the half-wavelength), R_{SW} does not depend on the value of L. Because SWs in the cranium cannot be avoided, modulations are necessary to reduce SWs (so as to lower R_{SW}).

In the case of single reflection of the monochromatic wave in this model, the amplitude is:

$$A_1(x) = \sqrt{1+2R\cos\left(\frac{4\pi}{\lambda}(L-x)\right)+R^2}. \qquad (5)$$

Although the average amplitude is different from that of multireflection, R_{SW} is the same as that of multireflection. In this model, multireflection increases the average amplitude, but does not change R_{SW}. In general, R_{SW} of single reflection is expected to be not so different from that of multireflection. We focus on the single-reflection experiment.

Modulation of the activation signal to the transducer

Generally speaking, an SW is generated when the transducer is activated by a sinusoidal wave. We compared the reduction in the SW around the center frequency of 500 kHz. We attempted to reduce the SW by modulating the sinusoidal wave using the three

random modulation methods described below. The signals are described by:

$$s(t) = A\sin[2\pi f_0 t + \phi(t)] \quad (6)$$

where A is the signal amplitude, f_0 is the carrier frequency of 500 kHz, and $\phi(t)$ is the phase angle function depending on the random modulation method.

FMN. Tang et al. used this method to eliminate the SW. This method induces a random phase shift in the sinusoidal wave by randomly changing the frequency around the carrier frequency. In this method, the derivative of the phase angle is given by noise:

$$d\phi_{FMN} = 2\pi N(t)dt \quad (7)$$

where the noise is represented by $N(t)$. The FMN has a parameter (*i.e.*, frequency deviation, D_f) that we set to be ±50 kHz (10% of the carrier frequency). As a result, $N(t)$ is noise uniformly distributed in the $[-D_f, D_f]$ range. In our experiment, we generated the FMN signal using the inner noise of the signal generator.

PSRF. We also used a new random modulation method, in which various frequencies are chosen periodically and the selected frequency is constant for a certain period T_{PSRF}. In this method, the derivative of the phase angle is expressed by:

$$d\phi_{PSRF} = 2\pi f_M(t)dt \quad (8)$$

where the value of $f_M(t)$ is changed to a random value between $-D_f$ (Hz) and $+D_f$ (Hz) every T_{PSRF} (s). An example of the waveform of the PSRF activation signal is shown in Figure 1a. The PSRF has two parameters: the length of period T_{PSRF} and the frequency deviation $\pm D_f$. We set the former to be 10 μs (five cycles of carrier) and the latter to be ±50 kHz (the same value as that for FMN) as a representative. In other words, every 10 μs, a different constant frequency was fed to the transducer to reduce the SW by a random frequency, even though the frequency component around the carrier frequency remained at a reasonable level. In our experiment, the SG reads the frequency values from a USB drive, in which we stored the data for the random values of frequencies.

RSBIC. The RSBIC method involves randomly selecting normal and inverse carrier phase signals by noise switching. In this method, the value of the phase angle $\phi_{RSBIC}(t)$ is either 0 or π. For the case in which $\phi = 0$, the signal belongs to the normal carrier, whereas for the case in which $\phi = \pi$, the signal belongs to the inverse carrier. The timing of switching between these carriers corresponds to the zero-cross timing of noise, the frequency bandwidth of which ranges from F_L (Hz) to F_U (Hz). Therefore, the timing of switching is random. An example of the waveform of the RSBIC activation signal is shown in Figure 1b. The RSBIC has two parameters: the lower cut-off frequencies of the noise F_L and the upper cut-off frequencies of the noise F_U. We set the former to be 50 kHz (10 cycles) and the latter to be 200 kHz (2.5 cycles) as representative values. In other words, the inverse carrier signal is chosen by activating a switching circuit with a zero-cross signal generated by noise, for which the frequency band has a range of 50–200 kHz. The SW is reduced by randomly superimposing an inverse phase signal, although the carrier component remained at a reasonable level. In our experiment, we used a custom-made circuit to generate the RSBIC signal.

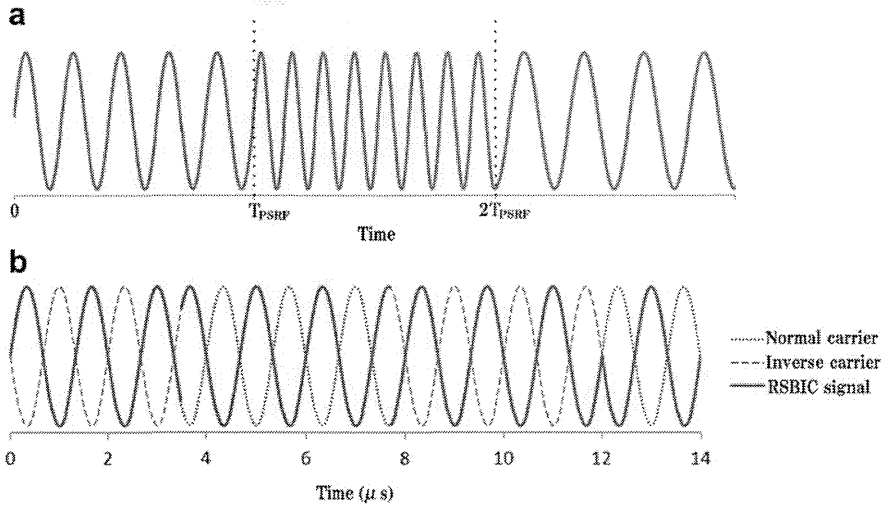

Fig. 1. (a) An example of the waveform of the PSRF activation signal. (b) An example of the waveform of the RSBIC activation signal.

The SWs obtained by the sinusoidal signal and the three random modulation methods mentioned here are compared using the schlieren method.

Schlieren observation

Figure 2 shows a diagram of the experimental setup. The SG (AFG3102; Tektronix, OR, USA) can generate a 500-kHz sinusoidal wave in addition to modulated waves. After the wave was amplified (HSA4101; NF Co., Yokohama, Japan) with an output impedance of 1.5 Ω + 0.5 μH, the wave was applied to a transducer consisting of a PZT. The shape of the transducer is a square with sides measuring 30 mm. The transducer has a nominal frequency of 500 kHz and a bandwidth of 350–750 kHz. Because the transducer is square, the free field generated by the transducer has fourfold symmetry. The applied wave was monitored using an oscilloscope (TDS3012; Tektronix). The transducer is situated in a water tank. A reflective plate was placed in the beam such that the plate was located 21 cm from the transducer surface and was reclined approximately 10 degrees to the horizontal plane to avoid complicated multireflection between the surface of the transducer and the reflective plate. The reflective plate was constructed of a 0.3-mm–thick copper plate attached to a 6.05-mm–thick acrylic plate. The reflection coefficient of the reflective plate was evaluated to be approximately 0.94 at a frequency of 500 kHz, which is greater than that of skull bone (approximately 0.6; Shimizu et al. 2012). An SW was generated by overlapping the reflected wave and the forward wave.

We used a schlieren device (US-250SL; Mizojiri Optical, Tokyo, Japan) to observe ultrasonic fields. The schlieren method has the advantages of not disturbing the ultrasonic fields and of measuring the spatial distribution in real time. As shown in the lower part of Figure 2, the device consists of a light source, two lenses, a water tank, and a charge-coupled device (CCD) camera. The light from the source passes through the first lens (*i.e.*, the water tank), and the second lens and is detected by the CCD camera. The schlieren device detects the difference in density based on the background density in the water. When an SW is generated, the antinodes are indicated as bright areas, and the nodes are indicated as dark areas in schlieren images. The duration of the brightness accumulation is approximately 0.08 s. After this reflective plate experiment, we placed the human skull in the same location as the plate and measured the SW caused by the temporal bone. All the human skull bones were purchased through the General Science Corporation Import Company (Tokyo, Japan) from Ets du Docteur Auzoux (Paris, France) on March 2006. The skull was cut into a ring having a width of approximately 4 cm. The human skull ring was stored in dry air and was immersed in ultrapure water for 2 days in advance. In our experiment, the transducer was located inside the skull ring, and the US was radiated from the transducer toward the inner surface of the skull ring (the temporal bone in particular). There was only one bone interface on the acoustic beam path. This experiment using human skull bone was approved by the institutional review board at the Jikei University School of Medicine, and all experimental procedures were performed in accordance with the rules of the ethical committee of the university.

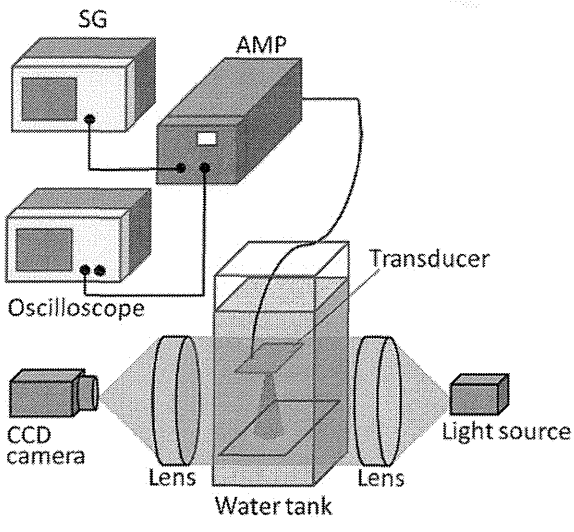

Fig. 2. Experimental setup.

Quantification of the effect of the SW reduction

Because there is a positive correlation between the gray scale in the schlieren images and the RMS value of acoustic pressure integrated along the light path, we can estimate the degree of SW reduction. In particular, a linear relationship has been demonstrated experimentally to exist between the brightness of the schlieren images and the input voltage of the activation signal when the input voltage is between 15 and 25 Vpp as a result of a preliminary verification. We used the range of voltage in which a linear relationship exists.

We quantify the effects of SW reduction using the ratio R_{SW} based on the brightness of the schlieren image. To calculate R_{SW}, we begin by selecting a rectangular region of interest (ROI) in schlieren images. Here, the longitudinal direction of the ROI is along the propagation direction of the wave, and the ROI includes several wavelengths. Next, the brightness distribution along the longitudinal direction is derived using freely available ImageJ software. At this time, the brightness is averaged along the lateral direction. From the

brightness distribution, the R_{SW} is calculated using the following formula:

$$R_{SW} = \frac{(B_{\text{local max}} - B_{\text{local min}})_{\text{Ave}}}{B_{\text{mean}}} \quad (9)$$

where $B_{\text{local max}}$, $B_{\text{local min}}$ and B_{mean} are the local maxima, the local minima and the mean of the brightness, respectively. The smaller the value of R_{SW}, the greater the reduction in the SW. R_{SW} depends on the location on the schlieren image; therefore, we selected three different ROIs in one schlieren image. The same location was used for each of the activation methods.

RESULTS

Frequency characteristics of the ultrasonic transducer

The frequency characteristics of the transducer used in the present study were measured using an acoustic intensity measurement system (AIMS; Onda corporation, Sunnyvale, CA, USA) with a hydrophone having a wide frequency bandwidth (100 kHz to 10 MHz). The spectra of the activation signal and the receiving signal as obtained by a hydrophone are shown in Figure 3. Comparison of the spectra reveals that the frequency characteristics of the transducer have a wide band of 350–750 kHz, as shown in Figure 3b.

Waveform and frequency spectrum for each activation signal

We show the waveform and frequency spectrum for each activation signal in Figure 4; these were monitored with an oscilloscope. The sinusoidal (SIN) signal has only a 500-kHz component. The waveform of the FMN signal is deformed slightly from an SIN wave, and its spectrum has components other than the 500-kHz component. In the case of the PSRF signal, we can see that the period is changed (*i.e.*, the rightmost period is shorter than the leftmost period) and the frequency is between 450 and 550 kHz. As shown in Figure 4g, phase reversal can be observed in the RSBIC signal. Note that the frequency spectrum of RSBIC is broader.

Using the hydrophone, we measured the wave emitted by the transducer for each of the activation methods. The resulting waveform and the frequency spectrum are shown in Figure 5. In the case of SIN activation, the spectrum of the emitted wave has only a 500-kHz component, as expected. In the case of FMN and PSRF activation, both the period and the amplitude are changed by the transducer response. The foot of the peak of the output frequency spectrum of FMN is slightly steeper than the input signal. The output spectrum of the PSRF has approximately the same shape as the input signal. The waveform is the most distorted in the RSBIC activation, which is promising for SW reduction. The output spectrum of RSBIC activation was changed from an input spectrum because of the transducer response.

The difference between the spectrum of the activation signal and the spectrum of the wave emitted by the transducer corresponds to the energy loss owing to the transducer response. In the case of FMN and PSRF, the input spectra do not have a much broader frequency band than the intrinsic bandwidth of the transducer, and the energy loss is low for these two methods. However, the energy loss is significant because the spectrum of RSBIC activation is broader than the intrinsic bandwidth of the transducer.

Quantitative measurement of electro-acoustic conversion

We measured the electric energy using a high-frequency watt meter (4410A; BIRD Technologies Group Electronic Corporation, OH, USA). When we activated the transducer with 20-Vpp SIN wave at 500 kHz, the electric energy was 600 mW. If the input voltage is 10 Vpp, the electric energy is estimated to be 150 mW. However, we measured the acoustic power using a hydrophone and calculated the spatially

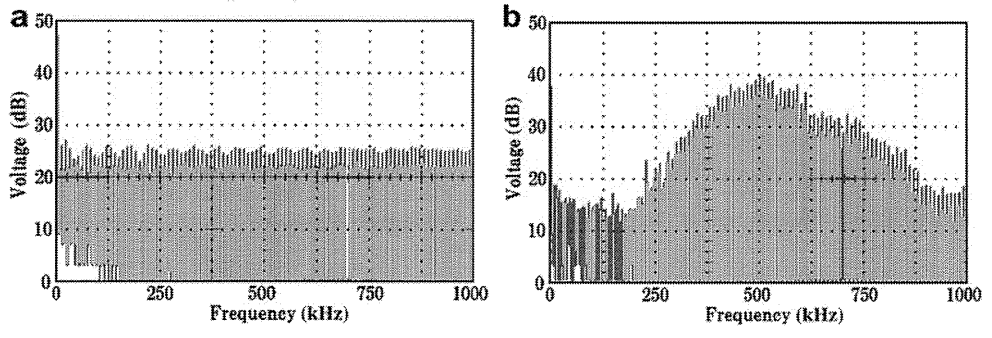

Fig. 3. Frequency characteristic of the transducer used in the present study. The duration of the time domain signals used to compute the spectra was 4 ms. We used the Hanning function. (a) Frequency spectrum of the activating wave. (b) Frequency spectrum of the receiving wave.

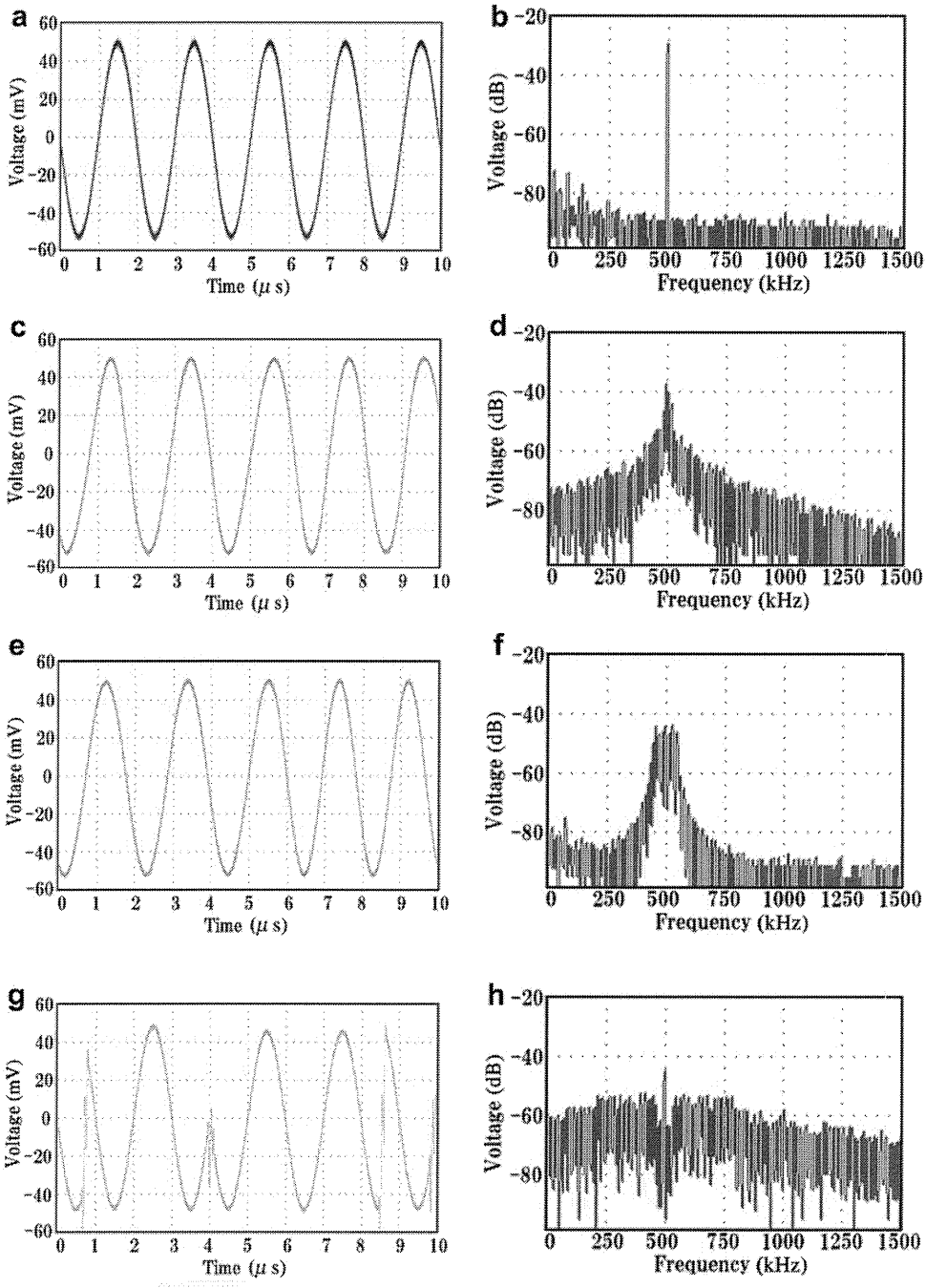

Fig. 4. Waveform and frequency spectrum for each activating signal. (a) Waveform of the SIN signal. (b) Spectrum of the SIN signal. (c) Waveform of the FMN signal. (d) Spectrum of the FMN signal. (e) Waveform of the PSRF signal. (f) Spectrum of the PSRF signal. (g) Waveform of the RSBIC signal. (h) Spectrum of the RSBIC signal. The carrier frequency was 500 kHz. The frequency deviation $\pm D_f$ was set to be ± 50 kHz for the FMN and PSRF signals. The length of section T_{PSRF} was 10 μs. The lower cut-off frequency of noise F_L was 50 kHz and the upper cut-off frequency of the noise F_U was 200 kHz for the RSBIC signal. The duration of the time signals used to compute the spectrum was 2 ms, and the Hanning function was used.

integrated acoustic power at the plane, which was parallel to the surface of the transducer (4 cm from the surface). When the activation voltage was 10 Vpp, the electric energy was 42 mW for SIN (520 kHz), 30 mW for SIN (500 kHz), 37 mW for FMN (500 ± 50 kHz), 35 mW for PSRF (500 ± 50 kHz, 10 μs), and 11 mW

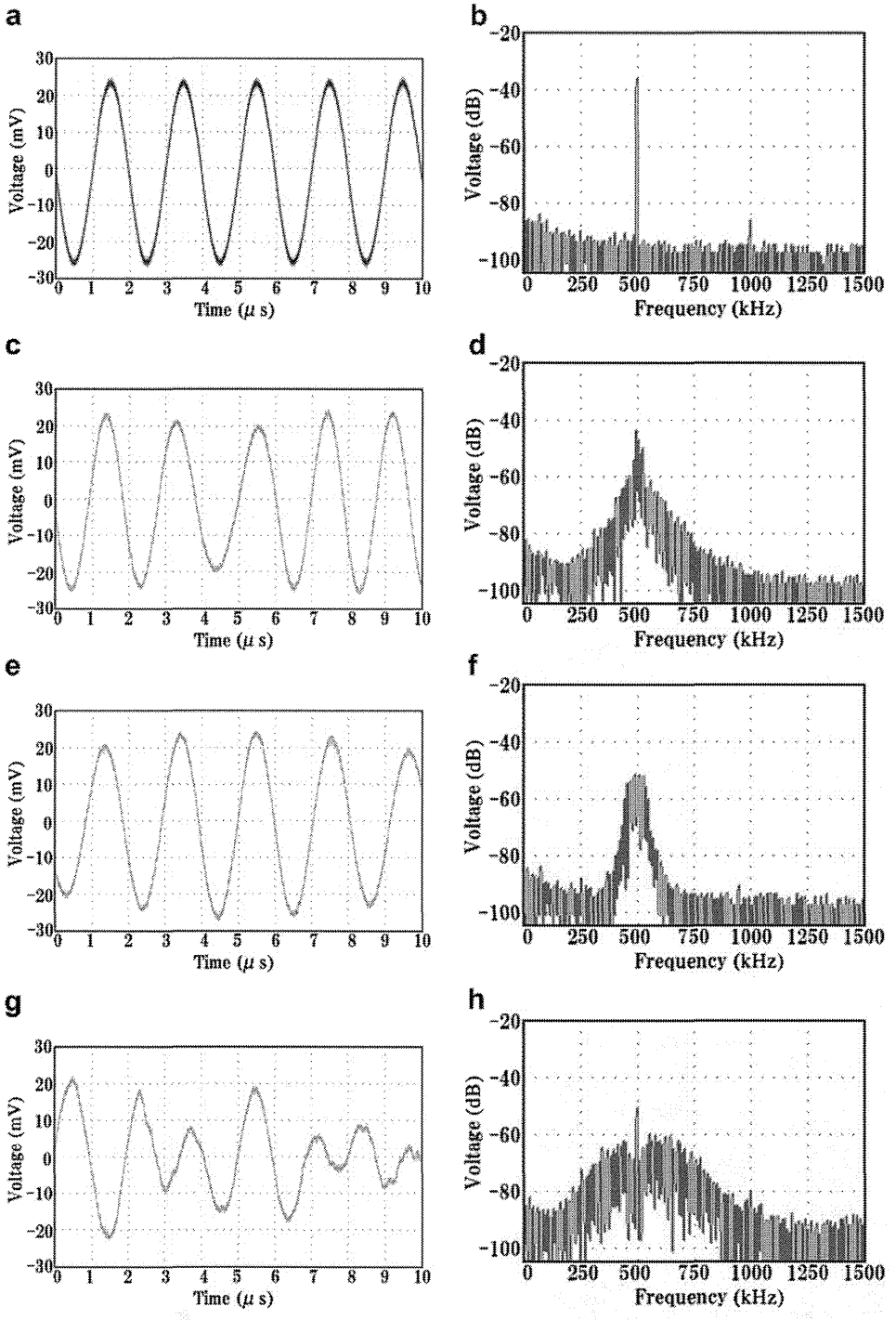

Fig. 5. Waveform and frequency spectrum of the wave emitted by the transducer. (a) Waveform activated by SIN. (b) Spectrum activated by SIN. (c) Waveform activated by FMN. (d) Spectrum activated by FMN. (e) Waveform activated by PSRF. (f) Spectrum activated by PSRF. (g) Waveform activated by RSBIC. (h) Spectrum activated by RSBIC. The hydrophone was located 8 cm from the center of the transducer. The activation voltage was 10 Vpp for all cases, and the carrier frequency was 500 kHz. The modulation parameters were the same as in Figure 4. The duration of the time signals used to compute the spectrum was 2 ms, and a Hanning function was used.

for RSBIC (500 kHz, 50–200 kHz). The acoustic energy produced by RSBIC is approximately one third of the SIN wave activation at 500 kHz. The part of the electric energy that is not converted to acoustic energy is used to raise the temperature of the transducer and corresponds to the energy loss.

Comparison of SW reduction between four different activation methods

Figure 6 shows the schlieren images obtained by the four different activation methods. The schlieren image was captured with a CCD camera (Fig. 2). In order to perform the R_{SW} calculations, we used three different ROIs, labeled A, B and C (Fig. 7). The same three regions were applied to each activation case.

Because the frequency characteristics of the transducer ranged from 350 kHz to 750 kHz (Fig. 3b), SWs were generated in this frequency bandwidth (Fig. 5), even though the activation signals to the transducer had a wide band over the transducer frequency response.

In the SIN case, light and dark stripes are clear in the schlieren image (Fig. 6a), which indicates the appearance of an SW. As expected, the distance between bright lines (antinodes) is 1.5 mm, which is approximately half the wavelength. The value of R_{SW} is 48%, 36% and 37%, in regions A, B and C, respectively.

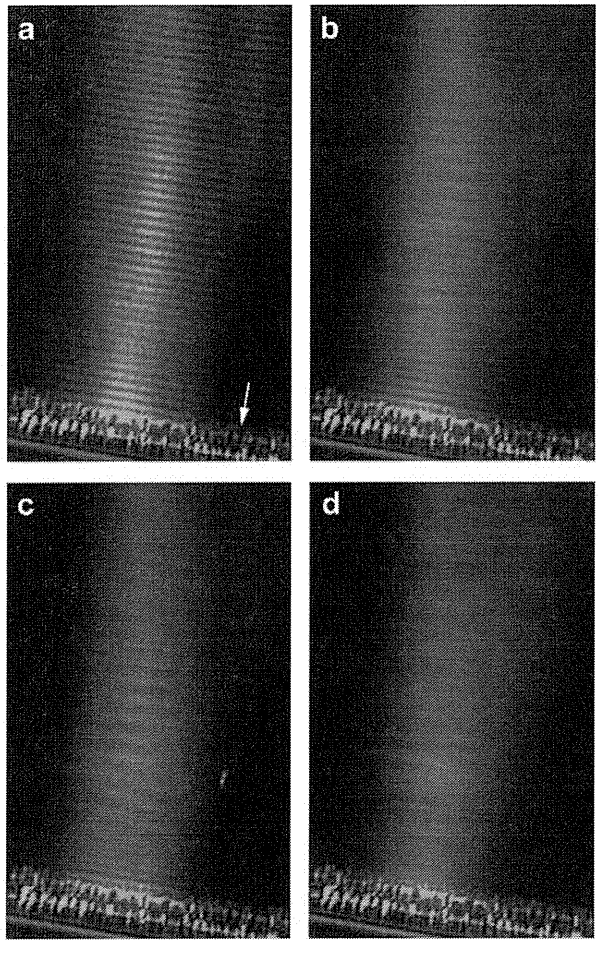

Fig. 6. Schlieren images obtained by the different activation methods. (a) SIN, (b) FMN, (c) PSRF and (d) RSBIC. The reflective plate is located in the lower part of the images (indicated by the white arrow). The activation voltage was 18 Vpp for the SIN, FMN, and PSRF signals and 24 Vpp for the RSBIC signal.

When we use FMN, the stripe is obscured (Fig. 6b) compared with SIN. Therefore, the SW is reduced. The value of R_{SW} is 11%, 24% and 12% in regions A, B and C, respectively. In the case of the PSRF, the SW reduction is clear in the schlieren image (Fig. 6c). The value of R_{SW} is 11%, 13% and 10% in regions A, B and C, respectively.

By RSBIC, we activated the transducer using a higher voltage (24 Vpp) because the power loss (the power that cannot be converted to the ultrasonic power from the electric power) was larger than in the other three activation methods. By increasing the voltage, we tried to maintain a constant average brightness, because we are not interested in the average brightness but rather in the R_{SW}. The brightness of the US wave is approximately uniform, and the SW reduction is obvious in Figure 6d. The value of R_{SW} is 5%, 4% and 6% in regions A, B and C, respectively.

The values of R_{SW} are listed in Table 1. In addition to R_{SW}, we calculated the ratio of R_{SW} to R_{SW} for the SIN case (rR_{SW}). The minimum R_{SW} appears in the activation signal of RSBIC in each ROI. The RSBIC has the potential to divide R_{SW} by a factor of 10. The value of R_{SW} varied with the selection of the location of the ROI, as shown, for example, for FMN and PSRF in ROI B and ROI C. In a comparative study, the selection of the ROI in the ultrasonic beam path is an important factor in evaluating R_{SW}.

Comparison of SWs generated by skull reflection

Figure 8 shows four SW patterns for schlieren images obtained from the four afore-mentioned activation methods. The R_{SW} was also calculated in one ROI indicated in Figure 8a by SIN activation. The location of this ROI was commonly used as an activation method for the R_{SW} calculations in Figure 8 (b–d). Note that the R_{SW} for the SIN wave was 25%, which is significantly lower than the value of R_{SW} from the flat reflection plate. The reason for this large reduction in R_{SW} is considered to be a distortion of the wave reflected from the inner surface of the curved skull. The random modulation activation methods showed a distinctly lower R_{SW} value than the SIN wave (Fig. 8a–d). However, the three random modulation methods did not generate as large a reduction in R_{SW} (Fig. 8b–d compared with Fig. 6b–d).

DISCUSSION AND CONCLUSIONS

In the present study on SW reduction methods, using a 1-D propagation model, we first clarified that the value of R_{SW} that appeared by multireflection can be estimated by the value of R_{SW} obtained using a single-plane

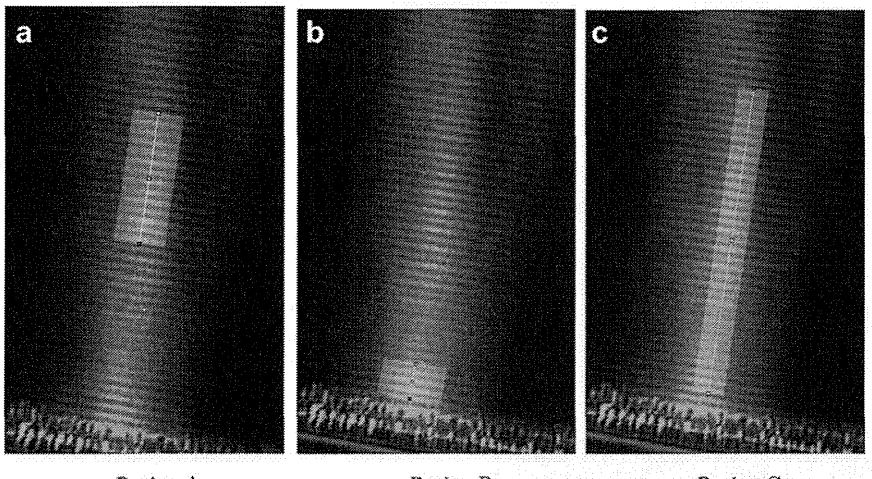

Fig. 7. Three ROIs considered in the present study. The value of R_{SW} was calculated separately in each ROI. These ROIs were used for the calculation in the schlieren images obtained using the four activation methods.

reflector. Next, the reduction of the effect of SWs caused by one reflection was experimentally compared under the condition of 500 kHz based on schlieren images for three types of random modulation methods of the transducer activation signal: FMN, new PSRF, and new RSBIC. The minimum R_{SW} of the schlieren images was obtained using RSBIC under the reflection conditions of a flat panel plate and the inner surface of the human skull.

Technical feasibility of the random modulation method: R_{SW} depending on the location of the ROI in the beam

The SW appeared nonhomogeneously, even in the far field of the ultrasonic beam, which was 11.25 cm from the transducer surface at the maximum frequency of 750 kHz for the 30 × 30-mm transducer. In addition, the plate is not orthogonal to the incident beam propagation axis, and diffraction occurs. Therefore, for the same ultrasonic beam, the value of the R_{SW} differs slightly depending on the choice of the ROI. Therefore, we selected three different ROIs in one beam, based on the acoustic field of the sinusoidal wave. We evaluated R_{SW} using the same ROI for each of the activation methods. The reason for the appearance of the inhomogeneity in the SW distribution is that the schlieren method provides a 2-D image by integrating the quantity of the reflection along the optical path through the 3-D distribution of the acoustic field and superimposing the traveling wave and the reflected waves. Therefore, the R_{SW} in ROI B in Figure 7 was considered to be a typical value indicating the SW reduction effect. Next, ROI A was selected as having a rather strong contrast in brightness between antinode and node locations with respect to the SW. As a result of selecting ROI A, the reduction effect was clearly demonstrated, as shown in Table 1. The minimum R_{SW} value was obtained in the random modulation of RSBIC in every ROI.

Table 1. Summary of R_{SW}

Activation method	R_{SW} (A)	R_{SW} (B)	R_{SW} (C)	rR_{SW} (A)	rR_{SW} (B)	rR_{SW} (C)
Sinusoidal	48%	36%	37%	1.0	1.0	1.0
FMN	11%	24%	12%	4.4	1.5	3.1
PSRF	11%	13%	10%	4.4	2.8	3.7
RSBIC	5%	4%	6%	9.6	9.0	6.2

FMN = frequency modulation by noise; PSRF = periodic selection of random frequency; RSBIC = random switching of both inverse carriers.

Comparison of results

Tang and Clement (2009, 2010) reported that randomization is important for the reduction of the SWs. In the present study, we confirmed their conclusion through the use of different experimental setups based on the schlieren method, which does not disturb the acoustic field. Furthermore, we found PSRF to be approximately equivalent to Tang's FMN and, at the expense of the narrow frequency band, RSBIC is superior to PSRF and FMN.

Tang and Clement (2010) reported that the quantity R, which corresponds to R_{SW} in the present study, was 0.063 for random modulation (FMN) and 0.354 for a single frequency of 250 kHz in their plastic chamber experiment. Thus, they reported that SWs were reduced by a factor of 5.6. In our experimental results (Table 1), FMN had a value of 4.4 in ROI A for rR_{SW}, 1.5 in ROI B, and 3.1 in ROI C. One possible explanation for this difference between data sets is the difference in the frequency spectrum, in which their spectrum has a high-frequency component that includes second

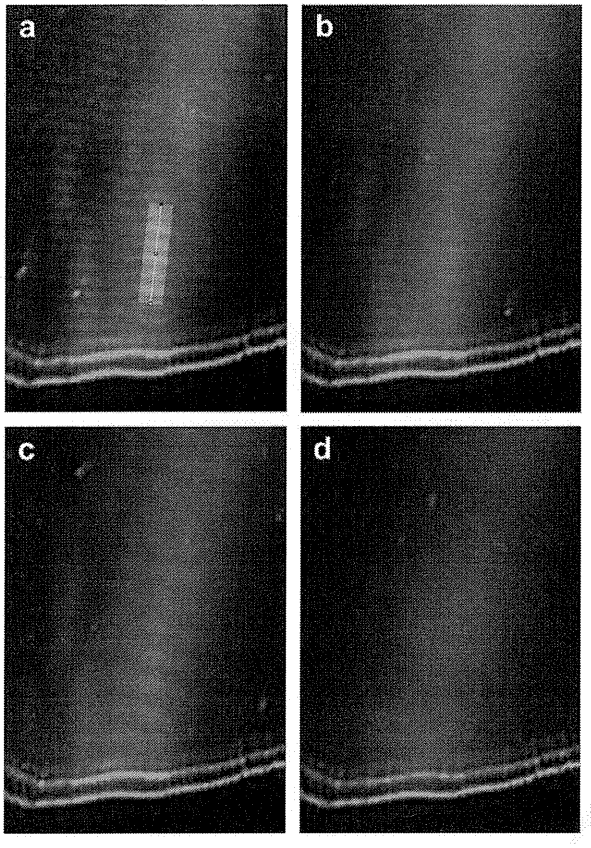

Fig. 8. Schlieren images obtained by four different activation methods: (a) SIN (R_{SW} = 25%; rR_{SW} = 1.0), (b) FMN (R_{SW} = 11%; rR_{SW} = 2.3), (c) PSRF (R_{SW} = 13%; rR_{SW} = 1.9) and (d) RSBIC (R_{SW} = 5%; rR_{SW} = 5). The activation voltages are 24, 24, 24 and 30 Vpp, respectively. The lower part of the images indicate the skull.

harmonics, which is more effective for reducing the appearance of the SW. On the other hand, the maximum frequency component of our noise spectrum was 1.5-fold larger than the carrier frequency of 500 kHz. An additional explanation for the difference in the SW reduction cannot be determined adequately based on their report.

Energy loss owing to transducer response

When we applied the RSBIC, we set the activation voltage to be 24 Vpp, which was larger than that in other cases, to maintain constant brightness for any activation method. The RSBIC has a lower energy conversion efficiency than other methods because, in such methods, a wide range of frequency components is generated (Fig. 4h). However, because the transducer did not have a sufficiently wide frequency response (Fig. 3b), the frequency response does not correspond to the spectrum of the activation signal. The difference between in frequency spectrum in Figs. 3b and 4h is not transducible to the acoustic power from the exciting electric power, and the loss induces transducer heating.

When we attempt to develop an instrument using the RSBIC, the energy loss should be taken into account so as not to induce thermal damage in the tissue near the transducer.

Loss of carrier frequency and reduction of SWs

Problems with SW reduction can be also clarified through frequency spectrum analysis to be a reciprocal relation between the carrier frequency components and random frequency power (Figs. 5 and 6). Ideally, the maximum frequency of the random spectrum is greater than twofold the carrier frequency. For example, in the case of the RSBIC, if we set the frequency band of the random switching to be broader, then R_{SW} decreases. At the same time, the 500-kHz component is decreased.

The loss of a strong carrier frequency can change the bioeffects through change in cavitation activity. As Chapelon et al. (1996) observed that pseudorandom phase-modulated CW signals could reduce cavitation activity, the random modulation methods used in the present study may play a role in preventing cavitation, even if cavitation is important for thrombolysis or BBB opening. Furthermore, according to Azuma et al. (2005), SWs reduce the cavitation threshold. Therefore, the random modulation will decrease the likelihood of cavitation through the reduction of SW in the transcranial ultrasonic therapy.

The trade-off between the carrier and the random power components can be defined based on the therapeutic effect, which required a suitable ratio of carrier and noise power in transcranial US. The results of the present study do not depend on actual clinical therapeutic technology; therefore, the degree of trade-off between the components can be derived through a biomedical study on the therapeutic effects and risk factors of tissue damage by SWs from a safety viewpoint.

Standing wave generation by the human skull

The SW pattern generated by the human skull bone remains unclear (Fig. 8), and each R_{SW} value is lower than that for the random modulation method (Fig. 8, Table 1). Lower R_{SW} is expected for the human skull because the reflection coefficient of bone is significantly lower than the reflection coefficient of the copper plate. Furthermore, the difference between the human skull bone and the flat-plane reflector is considered to occur for the following two reasons. First, since the inner surface of the skull has a three-dimensional curved surface with numerous small hills and valleys, the 3-D SW pattern that is formed has an onion-like structure. Second, based on the principle of the schlieren method, the 2-D brightness indicates the integration of the refraction component along the light beam line. Therefore, the SW pattern obtained by the schlieren method used in the